Clinical Infectious Diseases

MAJOR ARTICLE

Prefrontal Recruitment Mitigates Risk-Taking Behavior in Human Immunodeficiency Virus-Infected Young Adults

Robert X. Smith,[1] Anika Guha,[1] Florin Vaida,[2] Robert H. Paul,[3] and Beau Ances[1]

[1]Department of Neurology, Washington University in St Louis, Missouri; [2]Division of Biostatistics and Bioinformatics, University of California, San Diego; and [3]Missouri Institute of Mental Health, University of Missouri in St Louis

Background. Human immunodeficiency virus (HIV)–infected (HIV^+) young adults often engage in risk-taking behavior. However, the disruptive effects of HIV on the neurobiological underpinnings of risky decision making are not well understood.

Methods. Risky decision making, measured via the Iowa Gambling Task (IGT), was compared voxel-wise to resting cerebral blood flow (rCBF) acquired via arterial spin labeling. Separate topographical maps were obtained for HIV-uninfected (HIV^-; n = 62) and HIV^+ (n = 41) young adults (18–24 years old) and were compared to the full cohort of participants. For the HIV^+ group, rCBF was compared to recent and nadir CD4.

Results. IGT performance was supported by rCBF in 3 distinct brain regions: regions I, II, and III. The relationship between IGT performance and rCBF in HIV^+ individuals was most robust in region I, the ventromedial prefrontal and insular cortices. Region II contained strong relationships for both HIV^- and HIV^+. Region III, dorsolateral prefrontal and posterior cingulate cortices, contained relationships that were strongest for HIV^- controls. IGT performance was intact among HIV^+ participants with higher rCBF in either region I or region III. By contrast, performance was worse among HIV^+ individuals with lower rCBF in both regions I and III when compared to HIV^- controls ($P = .01$). rCBF in region III was reduced in HIV^+ compared with HIV^- individuals ($P = .04$), and positively associated with nadir CD4 cell count ($P = .02$).

Conclusions. Recruitment of executive systems (region III) mitigates risk-taking behavior in HIV^+ and HIV^- individuals. Recruitment of reward systems (region I) mitigates risk-taking behavior when region III is disrupted due to immunological compromise. Identifying individual recruitment patterns may aid anatomically directed therapeutics or psychosocial interventions.

Keywords. HIV; risky decision making; cerebral blood flow; plasticity.

Risk-taking behavior during young adulthood is a key contributor to human immunodeficiency virus (HIV) infection and unintentional injuries [1]. Increased risk-taking behavior during this developmental period has been linked to prefrontal control systems [2]. Two brain regions featured heavily in cognitive control studies include the dorsolateral prefrontal cortex (DLPFC) and ventromedial prefrontal cortex (vmPFC). The former is implicated in executive functions including attention and impulse control [3], whereas the latter plays a prominent role in reversal learning and emotional processing [4]. Severe damage to either region can lead to disastrous real-life decision making [5], pointing to a disruption in these underlying neurobehavioral systems. Neuroimaging results point to an interaction whereby the DLPFC enables long-term consideration during decision making by modifying intertemporal values framed by vmPFC activity [6]. In emotional contexts, this interaction manifests as self-control [7], a key component to risky decision making. However, modular approaches aimed at isolating the functions of specific cortical substrates are inherently limited at delineating the mechanisms of brain disruption at the systems level.

HIV enters the brain within weeks of infection, resulting in brain disruption. However, the neurobehavioral response to HIV infection is heterogeneous [8], suggesting that some HIV-infected (HIV^+) individuals may be resilient to its disruptive effects. The neural mechanisms governing disease response variability in HIV^+ individuals remain unclear. The neurobiological underpinnings of risky decision making in HIV^+ and HIV^- young adults can be evaluated using resting cerebral blood flow (rCBF), an imaging correlate of neuronal function. Risky decision making was assessed using the Iowa Gambling Task (IGT) [9]. Poor IGT performance reflects an impaired ability to identify and consistently utilize adaptive responses to avoid aversive consequences. Both poor IGT performance and reduced rCBF in cortical and subcortical brain regions have been reported previously among individuals with HIV-related cognitive impairment [10–12]. Prior structural neuroimaging studies have identified anatomical correlates of suboptimal performance on the IGT in HIV^+ individuals, but investigations have not examined the dynamic interplay of regional rCBF. Our focus on rCBF provides a unique opportunity to identify both

Received 3 July 2017; editorial decision 8 November 2017; accepted 17 November 2017; published online November 21, 2017.

Correspondence: B. Ances, Department of Neurology, Washington University, Box 8111, 660 South Euclid Ave, Saint Louis, MO 63110 (bances@wustl.edu).

Clinical Infectious Diseases® 2018;66(10):1595–1601

DOI: 10.1093/cid/cix1031

compromised and compensatory neural substrates of IGT performance in this population. Leveraging the spatial resolution of functional magnetic resonance imaging (MRI), we mapped the rCBF-IGT performance relationship across cortical and subcortical brain regions.

We hypothesized that the neuroimaging signature (defined by rCBF) of IGT performance would be unique in HIV^+ individuals compared to HIV^- individuals. Confirmation of this hypothesis could potentially guide the development and implementation of therapeutic targets (eg, transcranial stimulation).

METHODS

Participants

HIV^+ and HIV^- young adults (18–24 years old) were recruited from registries including the Supportive Positive Opportunities with Teens, and from the Infectious Disease Clinic and the AIDS Clinical Trial Unit at Washington University in St Louis. These sites reflect the general HIV^+ and HIV^- adolescent populations in the Saint Louis metropolitan area. Serologic status of all HIV^- participants was confirmed by the rapid oral HIV test at the time of testing. Participants were tested for tetrahydrocannabinol using a urine drug screen, and self-reported current tobacco use. Exclusion criteria included history of claustrophobia or seizures, previous head injury with loss of consciousness >30 minutes, developmental delay, psychiatric conditions associated with cognitive dysfunction, current alcohol or substance use disorder, depression (as assessed by a Beck Depression Inventory II score >29) [13], contraindications for MRI scanning (metal implants, pacemakers, etc), <8 years of education, and inability to provide written informed consent. For the HIV^+ group, clinical laboratory values (eg, current plasma viral load, current and nadir CD4 cell count) were obtained within 3 months of scanning. This study was approved by the Washington University in St Louis Institutional Review Board.

Imaging Protocol

All neuroimaging was performed on the same 3T Siemens Tim Trio MR scanner (Siemens AG, Erlangen, Germany) with a 12-channel head coil. A high-resolution, 3-dimensional, sagittal, magnetization-prepared rapid gradient echo scan T1 scan was acquired (repetition time [TR] = 2400 ms; echo time (TE) = 3.16 ms; flip angle = 8°; inversion time = 1000 ms; voxel size = 1 × 1 × 1 mm^3 voxels; 256 × 256 × 176 acquisition matrix; 162 slices).

A 2-dimensional multislice oblique axial spin density/T2-weighted fast spin echo scan (TE = 450 milliseconds; TR = 3200 milliseconds; 256 × 256 acquisition matrix; 1 × 1 × 1 mm voxels) was acquired for image registration. Pseudocontinuous arterial spin labeling (pCASL) was obtained (1.5 seconds labeling time; 1.2 seconds postlabeling delay; TR = 3500 seconds; TE = 9.0 milliseconds; 64 × 64 acquisition matrix; 90° flip angle; 22 axial slices with a 1-mm gap; and voxel size of 3.4 × 3.4 × 5.0). Two pCASL scans were acquired, with each containing 60 volumes (30 pairs of control and label volumes, duration of 3.5 minutes). rCBF values were computed for each control-label pair using a single compartment model [14]:

$$f = \frac{\lambda \Delta M R_{1a}}{2\alpha M_0 \left[\exp\left(-wR_{1a}\right) - \exp\left(-\left(\tau + w\right)R_{1a}\right)\right]}$$

where f is rCBF, R_{1a} (=0.606 $seconds^{-1}$ at 3 T) is longitudinal relaxation rate of blood, M_0 is the equilibrium magnetization of brain (control image intensity), α is the tagging efficiency (0.85), τ (18.4 ms × number of radiofrequency blocks) is the duration of the labeling pulse, λ is blood/tissue water partition coefficient (0.9 g/mL), and w is postlabeling delay time. Image preprocessing followed previously reported methods using in-house software [15]. For each participant, motion artifacts were managed using a 2-step process: (1) rigid registration to the mean volume was initially performed, and (2) estimated motion parameters from step 1 were used as weights in the calculation of mean rCBF = $\Sigma\alpha(i)*f(i)$, where α(i) is the weight determined from the motion parameters, and f(i) is the i-th rCBF volume. Mean rCBF for each participant was registered to a common atlas through a series of 3 linear registrations: (1) the mean control volumes were registered to corresponding T2 images, (2) T2 images were registered to a participant's T1 image, and (3) T1 images were registered to a common atlas.

Risky Decision-Making Performance

A computerized IGT was administered to all participants outside of the scanner. Four decks of cards were presented and participants were directed to select cards resulting in either a financial reward or financial penalty. Two of the decks resulted in larger rewards and penalties, while the other 2 decks resulted in smaller rewards and penalties. The total amount of money won or lost for each drawn card was displayed. The optimal strategy involved selecting cards from the "advantageous" smaller reward/penalty decks, and avoiding "bad" larger reward/penalty decks [9]. Participants were instructed to choose cards to maximize "winnings." A total of 5 blocks (20 selections per block) were administered.

Scores for each trial were calculated by subtracting the number of "bad" choices from the number of "advantageous" choices [16]. To examine whether participants shifted their strategy during the task to make better decisions (choosing the advantageous decks), an overall score was calculated by subtracting scores for the first block from the last block. This score was used for subsequent IGT analyses [17].

Analyses

We performed a multistep analysis: (1) We determined whether the spatial maps of rCBF-IGT performance differed by serostatus; (2) we evaluated whether rCBF within brain systems identified in step 1 were associated with HIV status; and (3) we

investigated whether changes in the relationship between brain systems identified in steps 1 and 2 reflected differences in IGT performance across HIV$^+$ individuals.

Demographics

Age, education, and IGT performance values were compared between groups using independent samples *t* tests. A χ^2 test was performed to examine sex and tobacco use differences between the 2 groups. Neither participant age nor sex was associated with IGT performance. However, total years of education was positively correlated with performance ($P = .001$).

CBF-IGT Association

Step 1: A simple linear regression model was used to adjust IGT performance and voxel-wise rCBF values for group differences in age, sex, education, and tobacco use. Residuals from these models were used in subsequent analyses. Voxel-wise associations of IGT performance and rCBF were computed within a gray matter mask using a Pearson correlation (Figure 1). Three separate rCBF-IGT relationship maps were obtained for HIV$^+$ and HIV$^-$ participants and the full cohort of participants (Figure 1). A cluster-based technique [18] was performed across gray-matter voxels to correct for multiple statistical comparisons using the RESTplus toolbox (version 1.2) [19]: (1) Random-effects maps, thresholded at $P < .05$, were permuted to compute a distribution of cluster size occurrence; (2) a minimum cluster size of 40 was determined based on a $P = .05$ occurrence threshold; (3) all significant voxels belonging to clusters smaller than this threshold were excluded. All 3 rCBF-IGT relationship maps were overlaid to identify common and exclusive regions (ie, regions occurring exclusively in either HIV$^+$ or HIV$^-$ maps). Region I contained clusters appearing in the HIV$^+$ map and not in the HIV$^-$ map. Region III contained clusters appearing exclusively in the HIV$^-$ map. Region II contained the remaining clusters.

rCBF Analyses

Step 2: The mean rCBF in regions I, II, and III was computed for all participants. Mean rCBF values were compared between groups using independent-samples *t* tests for each region. The association between IGT performance and mean rCBF values of regions I, II, and III were computed using a Pearson correlation. Correlation values were compared across groups using a Fisher *z* transformation.

HIV$^+$ Subgroups

Step 3: Regions I and III are consistent with previous studies investigating the neural substrates of IGT performance [4, 5, 9]. Neuroimaging studies have shown that the changes in the relationship between these regions modulate factors important to risky decision making such as self-control [6, 7]. We performed 2 sequential sets of analyses (Figure 2). First, we investigated whether the rCBF-IGT relationship in region I was modified by rCBF in region III. To do this, we used the median rCBF value for HIV$^-$ participants in region III to define a cutoff (C3 = 0.098). HIV$^+$ participants were subsequently classified into 2 groups, H3 (n = 14) and L3 (n = 27). H3 members had a mean rCBF in region III greater than C3, whereas L3 members were lower or equal to C3. We then investigated whether successful IGT performance (compared to HIV$^-$ controls) depended on rCBF in region III or region I. A separate cutoff was defined for region I from the median rCBF value for HIV$^-$ participants (C1 = 0.199). L3 members were further classified into 2 groups, H1 and L1. H1 members (n = 16) had a mean rCBF in region I greater than C1, whereas L1 members (n = 11) were lower or equal to C1.

The association between IGT performance and mean rCBF values of region I was examined using a Pearson correlation for the H3 and L3 subgroups. Correlation values were compared across the H3 and impaired subgroups using a Fisher *z* transformation. IGT performance values were compared between the H3, H1, L1, and HIV$^-$ groups using independent samples *t* tests. Both the current and nadir CD4 cell counts were compared between the H3 and L3 HIV$^+$ subgroups using independent-samples *t* tests.

RESULTS

Clinical Characterization of Participants

A total of 41 HIV$^+$ and 62 HIV$^-$ participants were evaluated. Demographic and clinical variables are summarized in Table 1.

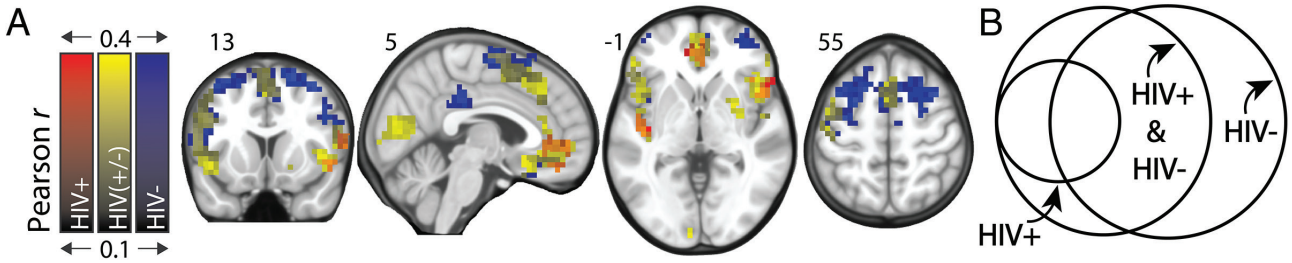

Figure 1. Iowa Gambling Task (IGT) performance is associated with resting cerebral blood flow (rCBF) within a distributed network of cortical and subcortical brain regions. *A*, Overlay of topological maps depicting IGT performance as a function of rCBF for human immunodeficiency virus–uninfected (HIV$^-$; n = 62) and human immunodeficiency virus–infected (HIV$^+$; n = 41) separately, and for the status-blind combination of HIV$^-$ and HIV$^+$ (n = 103). rCBF-IGT maps comprise voxels where rCBF significantly correlated with performance on IGT after cluster thresholding ($P < .05$). Scales denote Pearson correlation values. *B*, Venn diagram depicts the spatial relationships among the 3 maps.

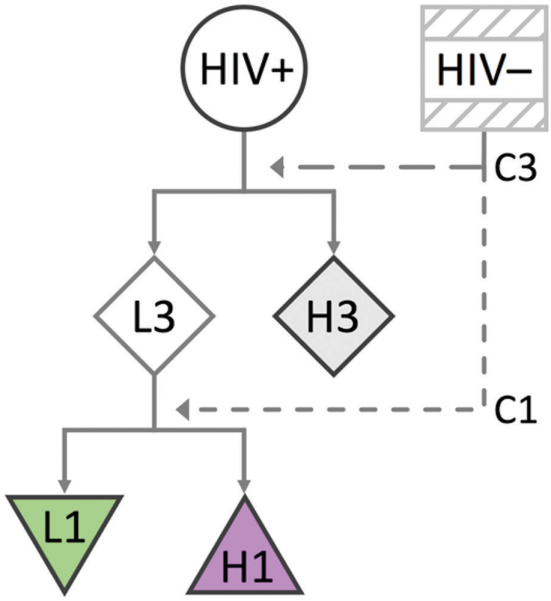

Figure 2. Flowchart of the sequential 2 steps defining the human immunodeficiency virus–infected (HIV$^+$) subgroups (H3, L3, H1, and L1). First, HIV$^+$ individuals are split into 2 subgroups, H3 and L3, based on their resting cerebral blood flow (rCBF) in region III. H3 members have rCBF values in region III greater than the median rCBF in region III for the human immunodeficiency virus–uninfected (HIV$^-$) group (C3). L3 members have rCBF values in region III less than C3. Second, L3 members are further split into 2 subgroups, H1 and L1, based on their rCBF in region I. H1 members have rCBF values in region I greater than the median rCBF in region I for the HIV$^-$ group (C1). L1 members have rCBF values in region I less than C1.

rCBF-IGT Relationship Maps

The brain regions that support adaptive risky decision making were evaluated by computing rCBF-IGT correlation maps for the HIV$^-$ and HIV$^+$ groups (Figure 1). We observed a broadly distributed network that composed of 3 neural systems (regions I, II, and III; Figure 3A and 3B). Region I was composed of the vmPFC and insula regions. Region II, the largest of the 3 systems, comprised of occipital and right putamen clusters, bilateral insular cortex, a frontal cluster extending across the presensorimotor area, and the dorsal anterior cingulate cortex. Region III was composed of bilateral clusters in the DLPFC and the posterior cingulate cortex, a brain region that has strong anterior to posterior connections [20]. The rCBF-IGT relationship progressively weakened from region I to region III for HIV$^+$ participants, but strengthened for HIV$^-$ individuals (Figure 3C).

Table 1. Demographic and Clinical Characteristics

Participant Characteristics	HIV-Uninfected (n = 62)	HIV-Infected (n = 41)
Age[a], y (SD)	21.4 (2.0)	22.3 (1.6)
Sex[a], % male	40	78
Education[a], y (SD)	13.3 (1.8)	12.6 (1.5)
Marijuana, %	37.1	26.8
Tobacco[a], %	32.2	65.8
Receiving HAART, %	…	87.1
Detectable viral load, % (>20 copies/mL)	…	51.4
Recent CD4 count, cells/μL (IQR)	…	492.7 (372.2–736)
Nadir CD4 count, cells/μL (IQR)	…	249.6 (207.2–436.2)

Abbreviations: HAART, highly active antiretroviral therapy, HIV, human immunodeficiency virus; IQR, interquartile range; SD, standard deviation.

[a]Significant group difference ($P < .05$).

Regional rCBF

To evaluate whether the anatomical shift in the rCBF-IGT relationship in HIV$^+$ participants corresponds to neurobiological changes, the average rCBF for regions I, II, and III was computed for all participants. We observed that region III rCBF was decreased ($P = .04$) for HIV$^+$ compared with HIV$^-$ participants (Figure 3D), suggesting impaired neuronal function. We also observed that rCBF in region III was negatively associated with rCBF in region I ($r = -0.34$, $P = .03$) for HIV$^+$ individuals (Figure 4A), whereas no relationship was observed for HIV$^-$ individuals.

Regional rCBF-IGT Relationship

Given the negative association between regions I and III in HIV$^+$ individuals, we predicted that reduced rCBF in region III would strongly modulate the rCBF-IGT relationship in region I. HIV$^+$ participants were classified as either having higher (H3, n = 14) or lower (L3, n = 27) rCBF in region III (see Methods). For HIV$^+$ participants, there was a significant difference ($P = .04$) in the strength of the rCBF-IGT relationship in region I between the L3 ($r = 0.72$) and H3 ($r = 0.24$) groups (Figure 4B).

IGT Performance

Consistent with previous work [10, 21], HIV$^+$ participants in our cohort performed significantly worse on the IGT compared with HIV$^-$ controls ($P = .02$). We evaluated whether recruitment of region I vs region III corresponded to IGT performance by categorizing HIV$^+$ participants into 1 of 3 groups (Figure 2): H3 (n = 14), H1 (n = 16), or L1 (n = 11). H3 participants had increased rCBF in region III. H1 participants had reduced rCBF in region III, but increased rCBF in region I. L1 participants had reduced rCBF in both region III and region I. We observed that IGT performance was significantly worse for L1 compared to H1 ($P = .01$), H3 ($P = .01$), and HIV$^-$ controls ($P = .01$). However, no difference in IGT performance was observed between H1 and H3 or to HIV$^-$ controls (Figure 4C).

Clinical Associations

The relationship between the observed neurobiological changes (reduced rCBF in region III) and common clinical variables associated with HIV-related injury were evaluated by comparing recent and nadir CD4 cell count values between the L3 and H3 groups. Nadir CD4 values were significantly reduced in L3 compared to H3 ($P = .02$; Figure 4D). However, no difference in recent CD4 was observed. No differences in nadir or recent CD4 cell count were observed between the L1 and H1 groups.

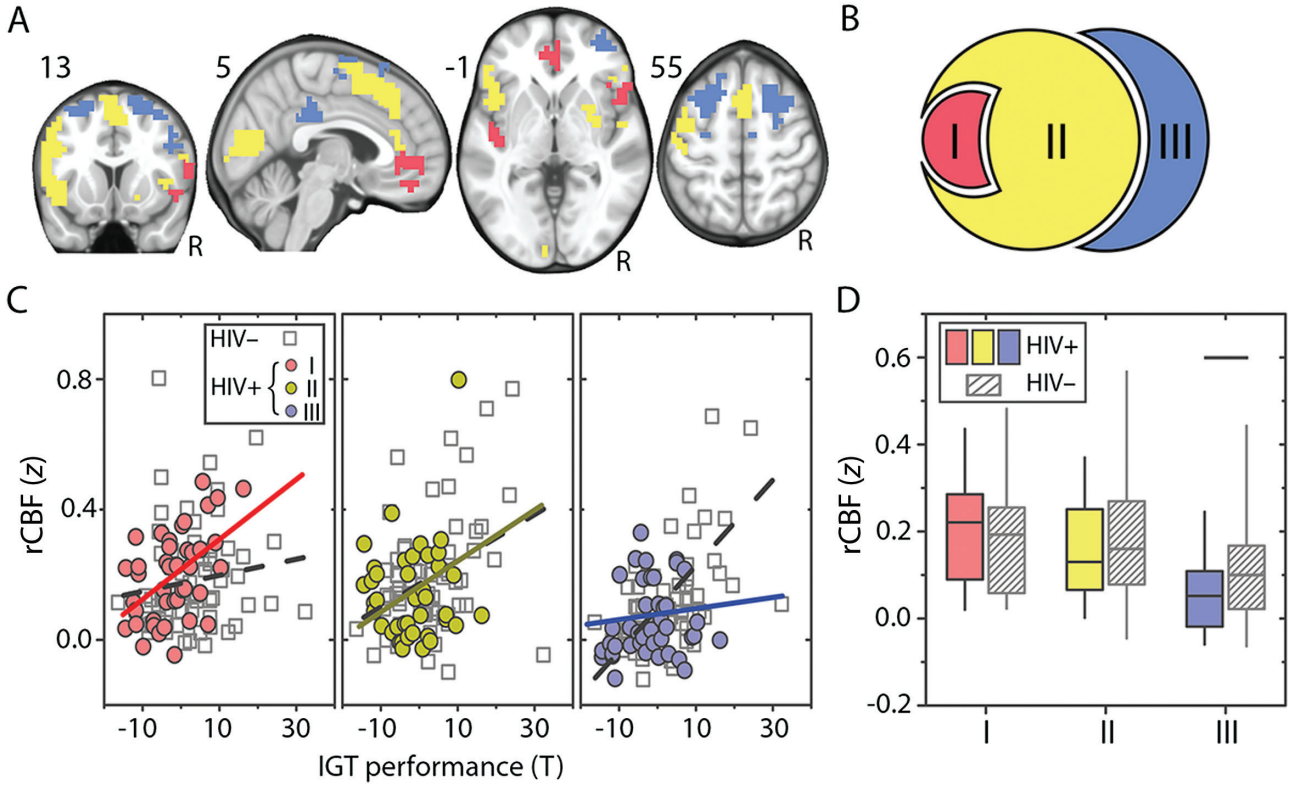

Figure 3. The spatial relationship between resting cerebral blood flow (rCBF) and Iowa Gambling Task (IGT) performance is associated with human immunodeficiency virus (HIV) status. *A*, Distinct brain territories where rCBF relates to IGT performance for HIV-infected (HIV^+) (region I), HIV-uninfected (HIV^-) (region III), and both HIV^+ and HIV^- young adults (region II). *B*, The parcellated Venn diagram (see Figure 1) depicts the boundaries for regions I, II, and III. *C*, rCBF-IGT relationship in each territory for HIV^- and HIV^+ young adults. *D*, Box plot of rCBF *z* score distribution percentiles (box: 25th–75th percentiles; whiskers: 5th–95th percentiles) for regions I, II, and III for HIV^+ and HIV^- (gray diagonal lines) participants. Horizontal black line denotes significant difference ($P = .04$).

DISCUSSION

Risk-taking behaviors in young adults may be more likely due in part to developmental heterogeneity between brain regions involved in impulse control vs emotional processing. Executive functions such as impulse control and attention develop slower throughout early adulthood, underscored by decreased DLPFC synaptic density [22]. In contrast, reward systems involved in emotional processing exhibit hyperresponsiveness throughout early adulthood [2]. We found that risky decision making in both HIV^- and HIV^+ young adults was supported by a large cortical and subcortical network of brain regions (region II) that mediate interactions between executive and reward systems [23]. However, risky decision making in HIV^- young adults further exhibited a strong reliance on executive systems (region III). Heavy reliance on executive systems in conjunction with slow maturation of these brain regions may place young individuals at increased risk for behavioral dysfunction due to HIV infection.

Our results provide insight into the disruptive effects of HIV infection on the brain. Previous studies have linked reduced CBF in prefrontal executive systems, including the DLPFC, and subcortical areas to cognitive impairment in HIV^+ adults [11, 12, 24]. We found that a subset of HIV^+ young adults (L3 group) who had brain disruption in executive systems also had a history of strong immunosuppression, as indexed by nadir CD4 cell count. This is consistent with prior reports that nadir CD4 cell count is associated with more severe cognitive impairment in HIV^+ [25]. Disruptions to the brain when the immune system is weak may contribute to cognitive impairment in HIV^+ individuals [26].

Dysfunction in executive systems typically complicates the decision-making process by impacting the ability to retain multiple pieces of information in short-term memory needed for forecasting and risk assessment. Here, however, brain disruption to executive systems did not necessarily associate with increased risky decision making, as indexed by decreased IGT performance. Instead we found that a subset of HIV^+ individuals (H1 group) with disruption to region III recruited a prefrontal network important for reward processing (region I) [27]. Conversely, a separate subset of HIV^+ young adults (L1 group) who did not recruit either executive or reward systems may be vulnerable to exogenous factors (eg, depression [28] or substance use [29]). These outcomes are consistent with predictions made by the somatic marker hypothesis, which states that emotions and visceral input from the sensory guide decision making [9]. This cross-sectional study focuses on the

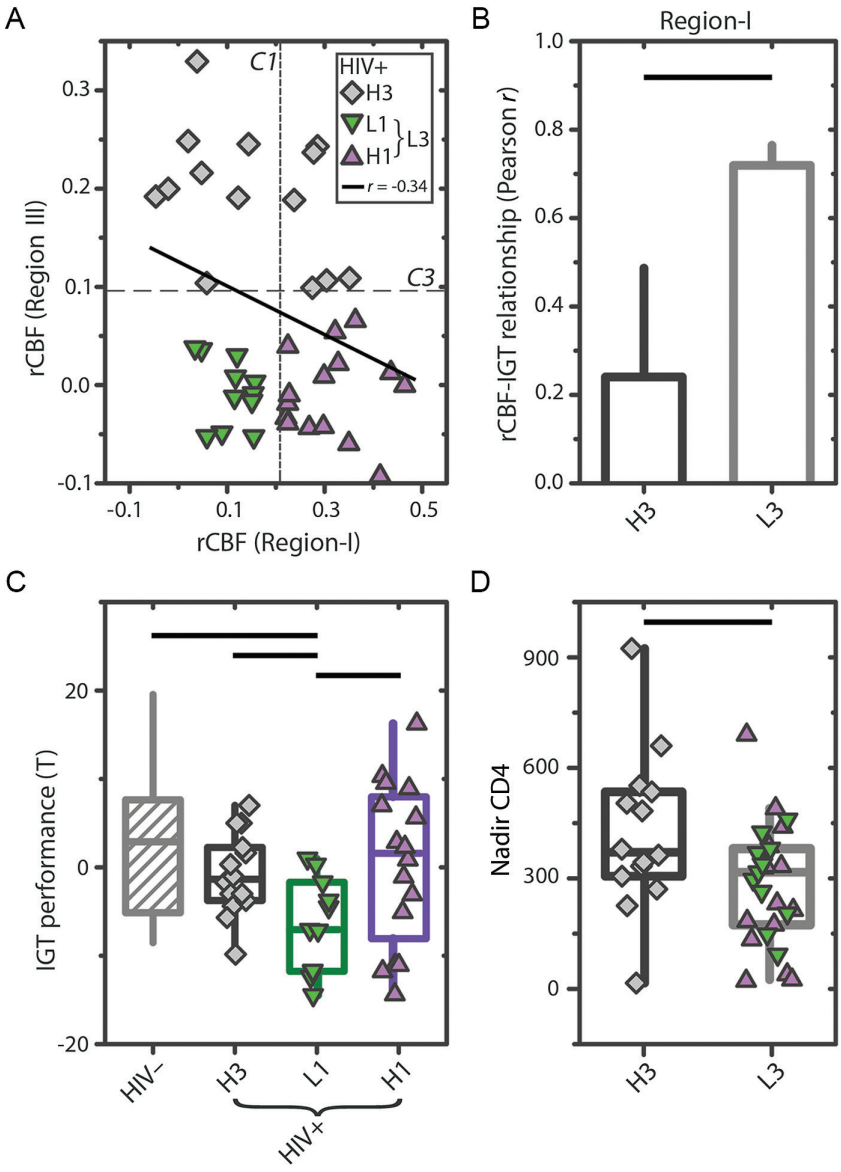

Figure 4. Three human immunodeficiency virus–infected (HIV$^+$) subgroups distinguished by resting cerebral blood flow (rCBF) in regions I and III are associated with Iowa Gambling Task (IGT) performance and historical severity of immunological suppression. *A*, Scatter plot showing the relationship between region I and region III for HIV$^+$ participants. The mean rCBF *z* scores of regions I and III were negatively associated ($r = –0.34$, $P = .03$) for HIV$^+$ participants. No association was observed for human immunodeficiency virus–uninfected (HIV$^–$) controls (not shown). Vertical and horizontal dashed lines indicate median rCBF values of regions I and III (C1 and C3), respectively, in HIV$^–$ controls. HIV$^+$ subgroups H3 (diamonds) and L3 (triangles and inverted triangles) are differentiated by C1. L3 subgroups H1 (triangles) and L1 (inverted triangles) are differentiated by C3. *B*, Bar plot showing Pearson correlation values between rCBF in region I and IGT performance for the H3 and L3 subgroups. *C*, Box plots of IGT performance for HIV$^–$ controls (diagonals), and HIV$^+$ subgroups (solid with symbols). *D*, Box plots of nadir CD4 cell count for HIV$^+$ subgroups H3 and L3. Horizontal black lines in (*B–D*) denote significant differences ($P < .05$).

heterogeneity in response to a specific cognitive demand that can be seen in HIV$^+$ individuals. Additional longitudinal studies are needed to specifically address the relationship between changes in cognition and rCBF within HIV$^+$ individuals.

The neurobehavioral response to HIV can be highly variable across individuals despite the prevalence of combined highly active antiretroviral therapy [30]. Observed variability may be partially explained by interindividual differences in utilizing executive systems (H3 vs L3 groups) and/or recruiting reward systems (H1 vs L1 groups). In the former case, early treatment and interindividual differences in immune response to HIV may be neuroprotective for executive systems. In the latter case, we found that in some individuals (H1 group), the brain remains relatively resilient to HIV despite a history of immunosuppression and insult to the DLPFC and posterior cingulate cortex, 2 critical hubs of the brain. These hubs enable efficient communication between different brain systems [31]. Damage to these brain regions may disrupt the balance of feedforward and feedback connections [32] that enable recurrent communication between systems [33], and can lead to behavioral dysfunction [4, 5, 9]. However, successful

risky decision making (ie, shifting from high- to low-risk/reward decks) is supported through recruitment of both the vmPFC, another critical hub, and parts of the insula. This may reflect inter-individual differences in the functional redundancy of executive and reward systems [34, 35]. Our results focused on young HIV$^+$ adults and need to be replicated in older chronically infected and virologically well-controlled HIV$^+$ individuals.

Our results have implications for the classification and treatment of individuals with HIV engaged in high-risk behavior. Based on these results, it may be possible to design a more precise therapy by identifying areas that have already been affected. Individuals identified with neural injury to executive systems (eg, H1 group) may benefit from psychosocial approaches such as cognitive behavioral therapy for attention deficits [36]. A combination of stimulants [37], psychosocial interventions, and neuromodulatory approaches, such as transcranial magnetic stimulation [38] and transcranial direct current stimulation [39] to the vmPFC, may help individuals with more widespread neural injury (eg, L1 group). These interventions may bolster integration of physical markers of potential threat and mitigate risk-taking behavior. Longitudinal studies of HIV$^+$ patients are needed to investigate the effectiveness of these forms of targeted intervention.

Notes

Acknowledgments. We express our sincerest gratitude to our study participants who helped make this work possible.

Financial support. This work was funded by the National Institutes of Health (grant numbers R01-NR012907, R01-NR012657, and R01-NR014449 to B. A.). Research was conducted and supported by the Washington University Institute of Clinical and Translational Sciences (award number UL1 TR000448 from the National Center for Advancing Translational Sciences) and in part by the Neuroimaging Informatics and Analysis Center (award number 1P30NS098577). R. X. S. has received funding from the Mount Sinai Institute for NeuroAIDS Disparities scholar program (award number R25MH080663).

Potential conflicts of interest. All authors: No reported conflicts. All authors have submitted the ICMJE Form for Disclosure of Potential Conflicts of Interest. Conflicts that the editors consider relevant to the content of the manuscript have been disclosed.

References

1. Kann L, McManus T, Harris WA, et al. Youth risk behavior surveillance—United States, 2015. MMWR Surveill Summ **2016**; 65:1–174.
2. Somerville LH, Jones RM, Casey BJ. A time of change: behavioral and neural correlates of adolescent sensitivity to appetitive and aversive environmental cues. Brain Cogn **2010**; 72:124–33.
3. Krawczyk DC. Contributions of the prefrontal cortex to the neural basis of human decision making. Neurosci Biobehav Rev **2002**; 26:631–64.
4. Wheeler EZ, Fellows LK. The human ventromedial frontal lobe is critical for learning from negative feedback. Brain **2008**; 131:1323–31.
5. Fellows LK, Farah MJ. Different underlying impairments in decision-making following ventromedial and dorsolateral frontal lobe damage in humans. Cereb Cortex **2005**; 15:58–63.
6. Hayashi T, Ko JH, Strafella AP, Dagher A. Dorsolateral prefrontal and orbitofrontal cortex interactions during self-control of cigarette craving. Proc Natl Acad Sci U S A **2013**; 110:4422–7.
7. Hare TA, Camerer CF, Rangel A. Self-control in decision-making involves modulation of the vmPFC valuation system. Science **2009**; 324:646–8.
8. Clifford DB, Ances BM. HIV-associated neurocognitive disorder. Lancet Infect Dis **2013**; 13:976–86.
9. Bechara A, Damasio AR, Damasio H, Anderson SW. Insensitivity to future consequences following damage to human prefrontal cortex. Cognition **1994**; 50:7–15.
10. Iudicello JE, Woods SP, Cattie JE, Doyle K, Grant I; HIV Neurobehavioral Research Program Group. Risky decision-making in HIV-associated neurocognitive disorders (HAND). Clin Neuropsychol **2013**; 27:256–75.
11. Ances BM, Sisti D, Vaida F, et al; HNRC Group. Resting cerebral blood flow: a potential biomarker of the effects of HIV in the brain. Neurology **2009**; 73:702–8.
12. Ances BM, Roc AC, Wang J, et al. Caudate blood flow and volume are reduced in HIV+ neurocognitively impaired patients. Neurology **2006**; 66:862–6.
13. Beck AT, Steer RA, Brown GK. Manual for the Beck Depression Inventory-II. Psychol Corp **1996**; 1–82.
14. Wang J, Zhang Y, Wolf RL, Roc AC, Alsop DC, Detre JA. Amplitude-modulated continuous arterial spin-labeling 3.0-T perfusion MR imaging with a single coil: feasibility study. Radiology **2005**; 235:218–28.
15. Tanenbaum AB, Snyder AZ, Brier MR, Ances BM. A method for reducing the effects of motion contamination in arterial spin labeling magnetic resonance imaging. J Cereb Blood Flow Metab **2015**; 35:1697–702.
16. Burdick JD, Roy AL, Raver CC. Evaluating the Iowa gambling task as a direct assessment of impulsivity with low-income children. Pers Individ Dif **2013**; 55:771–6.
17. Li X, Lu ZL, D'Argembeau A, Ng M, Bechara A. The Iowa gambling task in fMRI images. Hum Brain Mapp **2010**; 31:410–23.
18. Forman SD, Cohen JD, Fitzgerald M, Eddy WF, Mintun MA, Noll DC. Improved assessment of significant activation in functional magnetic resonance imaging (fMRI): use of a cluster-size threshold. Magn Reson Med **1995**; 33:636–47.
19. Song XW, Dong ZY, Long XY, et al. REST: a toolkit for resting-state functional magnetic resonance imaging data processing. PLoS One **2011**; 6:e25031.
20. Buckner RL, Andrews-Hanna JR, Schacter DL. The brain's default network: anatomy, function, and relevance to disease. Ann N Y Acad Sci **2008**; 1124:1–38.
21. Hardy DJ, Hinkin CH, Levine AJ, Castellon SA, Lam MN. Risky decision making assessed with the gambling task in adults with HIV. Neuropsychology **2006**; 20:355–60.
22. Petanjek Z, Judaš M, Šimic G, et al. Extraordinary neoteny of synaptic spines in the human prefrontal cortex. Proc Natl Acad Sci U S A **2011**; 108:13281–6.
23. Menon V, Uddin LQ. Saliency, switching, attention and control: a network model of insula function. Brain Struct Funct **2010**; 214:655–67.
24. Chang L, Ernst T, Leonido-Yee M, Speck O. Perfusion MRI detects rCBF abnormalities in early stages of HIV-cognitive motor complex. Neurology **2000**; 54:389–96.
25. Ellis RJ, Badiee J, Vaida F, et al; CHARTER Group. CD4 nadir is a predictor of HIV neurocognitive impairment in the era of combination antiretroviral therapy. AIDS **2011**; 25:1747–51.
26. Kore I, Ananworanich J, Valcour V, et al; RV254/SEARCH 010 Study Group. Neuropsychological impairment in acute HIV and the effect of immediate antiretroviral therapy. J Acquir Immune Defic Syndr **2015**; 70:393–9.
27. Craig AD. How do you feel—now? The anterior insula and human awareness. Nat Rev Neurosci **2009**; 10:59–70.
28. Krishnan V, Nestler EJ. The molecular neurobiology of depression. Nature **2008**; 455:894–902.
29. Lüscher C, Malenka RC. Drug-evoked synaptic plasticity in addiction: from molecular changes to circuit remodeling. Neuron **2011**; 69:650–63.
30. Heaton RK, Clifford DB, Franklin DR Jr, et al; CHARTER Group. HIV-associated neurocognitive disorders persist in the era of potent antiretroviral therapy: CHARTER Study. Neurology **2010**; 75:2087–96.
31. Jeong H, Tombor B, Albert R, Oltvai ZN, Barabási AL. The large-scale organization of metabolic networks. Nature **2000**; 407:651–4.
32. Laje R, Buonomano DV. Robust timing and motor patterns by taming chaos in recurrent neural networks. Nat Neurosci **2013**; 16:925–33.
33. Smith RX, Jann K, Ances B, Wang DJ. Wavelet-based regularity analysis reveals recurrent spatiotemporal behavior in resting-state fMRI. Hum Brain Mapp **2015**; 36:3603–20.
34. Albert R, Jeong H, Barabasi AL. Error and attack tolerance of complex networks. Nature **2000**; 406:378–82.
35. Achard S, Salvador R, Whitcher B, Suckling J, Bullmore E. A resilient, low-frequency, small-world human brain functional network with highly connected association cortical hubs. J Neurosci **2006**; 26:63–72.
36. Knouse LE, Safren SA. Current status of cognitive behavioral therapy for adult attention-deficit hyperactivity disorder. Psychiatr Clin North Am **2010**; 33:497–509.
37. Kempton S, Vance A, Maruff P, Luk E, Costin J, Pantelis C. Executive function and attention deficit hyperactivity disorder: stimulant medication and better executive function performance in children. Psychol Med **1999**; 29:527–38.
38. Parkin BL, Ekhtiari H, Walsh VF. Non-invasive human brain stimulation in cognitive neuroscience: a primer. Neuron **2015**; 87:932–45.
39. Jog MV, Smith RX, Jann K, et al. In-vivo imaging of magnetic fields induced by transcranial direct current stimulation (tDCS) in human brain using MRI. Sci Rep **2016**; 6:34385.